*Egypt. J. Chem.* **Vol. 65**, No. 6. pp. 741 - 752 (2022)

**Egyptian Journal of Chemistry**

**http://ejchem.journals.ekb.eg/**

# Hydrothermal Synthesis and Application of Nanocomposite as a Demulsifier in Crude Oil Processing

***Naeem A. Basher , **Ali Abdulkhabeer Ali**

*college of Science - Chemistry department/ University of Thi-Qar/ Iraq.

** College of Science - Chemistry department / Marshes research center- University of Thi-Qar/ Iraq .

E-mail: nae.abd_ch@utq.edu.iq

*Corresponding Email: aranru79@utq.edu.iq*

**Abstract:** In the present study, the nanocomposite demulsifiers $Fe_2O_3.B_2O_3$-[TBIP] was used to dehydrate crude oil. A superhydrophilicdemulsifier was created by functionalizing nanoparticles with [TBIP] thiadiazole derivative to improve their hydrophobicity and hydrophilicity.Thestructural characteristics and morphology of the prepared nanodemulsifier were investigated by (FT-IR), $^1$H-NMR, (XRD), (AFM), (FESEM) and (TEM).A bottle test was also used to assess the performance of the nanodemulsifier. The bottle test results revealed that nanocomposite has the highest nanodemulsifier efficiency, and crude oil reduction was accomplished in 90 minutes. Furthermore, the impacts of temperature and concentration revealed that both elements influence the stability of water in an oil emulsion. The separation efficiency of the prepared nanocomposite $Fe_2O_3.B_2O_3$-TBIP was compared with that of the commercial demulsifier (RP96BQ), used in the oil field and under the same conditions. The demulsification percentage of the prepared nanocomposite was (79.3 %) while the commercial demulsifier reached (86.2 %).

Keywords: Crude oil, nanodemulsifier, demulsification process , hydrothermal method ,$Fe_2O_3.B_2O_3$-TBIP

## 1. Introduction

Nanoscience and nanotechnology are primarily concerned with synthesis, Nanostructured materials description, exploration, and exploitation. These materials are characterized by at least one nanometer (1nm=$10^{-9}$ m) dimension[1]. As expressed by popular belief, applying these advanced technologies will assist humanity in solving global challenges linked to the supply of food, fuel, and energy, overcome deadly diseases,and develop great information and communication technologies [2].Demulsification can be accomplished in three ways: physically, chemically, orbiologically. It has been used to separate oil and water using gravity and centrifugal separations, as well as chemical treatment, flotation, filtration, membrane processes, evaporation, activated carbon adsorption, biological treatment, and integrated or hybrid processes all over the world. It was recently proved that using aerogels, magnetic materials, and fluorosurfactant polymers could improve oil/water separation processes [3].Severalexperiments have been conducted to show that adding nanoparticles to surfactants reduces surfactant adsorption on the walls of pores, thus boosting surfactant efficiency. The addition of nanocomposites at concentrations lower than the surfactant's critical micelle concentration has been demonstrated to drastically diminish surfactant adsorption as well as theinterfacial *tension*(IFT) between brine and oil[4] .$Fe_3O_4$nanocomposites were made by TianwenMi and her team in 2020 [5] , They

DOI: 10.21608/EJCHEM.2022.117673.5304

were used to develop a faster method of removing very small oil droplets from hexadecane/water emulsions,The researcher has studied , They were used to develop a faster method of removing very small oil droplets from hexadecane/water emulsions. The researchers studied humic acid and polydimethyldiallyl ammonium chloride-coated $Fe_3O_4$ nanoparticles that were created in a single location. Making the nano metal particles was a breeze. They were also quite good at separating oil from water, which means they might be used extensively to treat emulsified oil wastewater.The purpose of this research is to create a new nanocomposite $Fe_2O_3.B_2O_3$-[TBIP], characterize it, and evaluate its efficacy as a demulsifier in crude oil processing.The efficiency of demulsifiers produced from nanocomposites surfactants in separation wasexamined. When a synthetic demulsifier is compared to a commercial demulsifier (RP96BQ),considering many aspects that directly affect the percentage of water separated. These factors are as follows: (i) Concentration of demulsifier (ii) Temperature effect (iii) Time effect**.**

## 2. **2. Materials and methods**:

### 3. 2.1. Material

All the laboratory chemicals used in this work are of high purity and come from well-known international companies. Table (2.1) shows the chemicals used in this study to prepare the nanocomposite and the processed companies**:**

### 2.2. Preparation of corrosion inhibitor $Fe_2O_3.B_2O_3$-[TBIP]nanocomposite

#### 2.2.1. Synthesis of iron borate nanoparticles $Fe_2O_3.B_2O_3$

The $Fe_2O_3$-$B_2O_3$ nanoparticles were made using a modified method for Vu T Tan et al., 2020 **[6].** In a typical synthesis, after dissolving 0.01 mole of aluminum acetate in 100 ml of water, 0.02 mole of urea is added to the solution with magnetic stirring. The mixture was then hydrothermally treated for 12 hours at a temperature of 80 °C. The acidity of the solution is reached (pH = 4) .The Fe $(OH)_3$sediment washed the with water and dried it for several hours in a 60°C oven.Iron oxide nanoparticles agglomerate when the product is heated to a temperature of up to 250 °C in the air. The nano-iron borates were synthesized using the primary precursor $Fe_2O_3$ nanoparticles in a single precipitation step. 200 ml of distilled water was mixed with boric acid $H_3BO_3$ and $Fe_2O_3$ nanoparticles in a typical synthesis. The molar ratio of $H_3BO_3$ to $Fe_2O_3$ is one to three .The mixture was agitated at a constant room temperature to ensure complete deposition of iron borate. Synthesis can take anywhere between (3 and 6 )hours. After the reaction, the white precipitate of iron borate was rinsed multiple times with distilled water. The $Fe_2O_3.B_2O_3$ particles were then dried for 15 hours in a 50°C oven. Some physical properties of $Fe_2O_3.B_2O_3$ nanoparticles:Chemical Formula($Fe_2O_3.B_2O_{3)}$, Molecular weight (229.304g/mol ),Color(Brown), Physical body (Solid powder) and Yield (85%) .

### 22.2.Preparation compound [TBIP]

In 100 ml of ethanol, potassium hydroxide (0.3 moles) has been dissolved. Carbon disulfide (16 mL) was added to the solution, then heated for 24–30 hours reflex. Chromatography is used to keep track of the reaction (TLC). Chill the result and add 10% hydrochloric acid to the reaction mixture. We will notice yellow crystals of the thiadiazole derivative form. The precipitate was filtered, washed, and recrystallized using water and ethanol. The melting point is [163–165] $^oC$**[7],** as shown in scheme (2–1).Mix (0.01) of the compound $(X_1)$ with (0.02) of hydrazine in the reaction vessel (Reflex) for 10-12 hours while continuing the reaction monitoring with (TLC). The product is filtered, washed, and recrystallized with ethanol and water. As a result, yellowish-white crystals with a high yield (78%) and fusion temperature are produced (195-200 $^oC$) **[8]**.The reaction is depicted in scheme (2-1) . Compound $(X_3)$ was obtained by mixing (0.02 mol) of 2,5-dihydroxybenzaldehyde dissolved in 50 mL of 100% ethanol with (0.01 mol) of the combination $(X_2)$, followedby3-4 drops of glacial acid ($CH_3COOH$), and (Reflex) for 3-4 hours. Cool the product to room temperature, filter the precipitate, and recrystallize it with ethanol and water toobtain a dark brown powder. The product percentage is roughly 80% at a fusiontemperature of 200–205 °C **[7],**As seen in scheme (2.1) .Anhydrous sodium carbonate (0.025 mol) was added to a solution of $(X_3)$ (0.01 mol) and 1-bromoeicosane (0.02 mol) in (15 mL) of DMF, andthe reaction mixture was raised by reflex for four hours, then cooled to a temperature of (-10) and left overnight.The precipitate [TBIP] is

washed and recrystallized to obtain it. At a fusion temperature of 100–105 °C, the light brown crystals have a yield of 90% **[9]**is depicted in scheme (2.1). Chemical formula ($C_{56}H_{94}N_6O_4S$), molecular weight (947.466), color (light brown), physical body (solid), and yield (90%) are some of the physical parameters of compound [TBIP].

### 2.2.3 Synthesis $Fe_2O_3.B_2O_3$-[TBIP] nanocomposite

First, 0.01 mole of dried $Fe_2O_3.B_2O_3$ and 0.01 mole of [TBIP] compound were suspended in 20 mL of ethanol. For 12 hours, the mixture was refluxed at 60°C. Filtering was used to collect the products, which were then rinsed many times with ethanol **[5]**. As it turns out, in scheme (2.1). Chemical Formula ($Fe_2B_2C_{52}H_{86}O_{10}N_6S$), M.Wt (1176.77), Color (dark brown), Physical Body (solid powder), and Yield (90%) are some of the physical properties of $Fe_2O_3.B_2O_3$-[TBIP] nanocomposite.

### 2.3. Composition andMorphological characteristics of $Fe_2O_3.B_2O_3$-[TBIP]

Atomic Force Microscopy (AFM) and X-ray diffraction (XRD, X'pert PW1730, Philips, US) were used to examine the crystal structure of the as-prepared iron boratesnanoparticles and $Fe_2O_3.B_2O_3$-[TBIP] nanocomposite. XRD patterns ranging from 10 to 90° were collected. The KBr pellet method was used to acquire (FT-IR) and (**$^1$**H-NMR). Particle preparation and morphology were investigated using SEM and TEM.

### 2.4.Demulsifier Preparation and Bottle Tests

Bottle testing is used to evaluate the efficiency of a demulsifier in a series of experiments that are designed to be as close as feasible to the conditions present in the actual production system**[10]**. Used crude oil emulsion from the Halfaya oil field was distributed in glass tubes (capacity tube: 10 ml), with one of them placed in a water bath at 30 °C and 60 °C for 90 minutes, with separate readouts (five readouts). The separation effectiveness of demulsifiers made from $Fe_2O_3.B_2O_3$-[TBIP] surfactant was investigated and compared to that of a commercial demulsifier (RP96BQ).

## 3. Results and discussion :

### 3.1.1. Atomic Force Microscopy (AFM)

In addition to determining the particle size distribution, the estimated 2D and 3D views of AFM images of $Fe_2O_3.B_2O_3$ nanoparticles were determined. Fe2O3-B2O3 nanoparticles The topographic features of the layers $Fe_2O_3.B_2O_3$ are depicted in 2D and 3D pictures in Figure (3.1). The two varieties appear to have very smooth surfaces with grains approximately the same size as the beginning nanopowder (20–30 nm).

### 3.1.2. XRD Analysis of $Fe_2O_3.B_2O_3$ and [TBIP]-$Fe_2O_3.B_2O_3$

The X-ray diffraction pattern of both $Fe_2O_3.B_2O_3$ and [TBIP]- $Fe_2O_3.B_2O_3$nanocomposite as shown in Fig.3.1 ( a- b) indicated that the main phase of both samples. The diffraction pattern of $Fe_2O_3.B_2O_3$nanocomposites showed seven sharp peaks at (18.6°), ( 30.5°) ,( 36.0°), (37.6°),( 43.6°),( 54.1°),( 57.5°), ( 63.3°), (71.7°) and (74.8°) corresponding to (88),( 542),( 2111),( 146),( 517),( 231), ( 630),( 1110), ( 77), (152) of $Fe_2O_3.B_2O_3$. The crystalline size of $Fe_2O_3.B_2O_3$ and [TBIP]-$Fe_2O_3.B_2O_3$ nanocompositewas calculated by Debye-Scherrer equation **[11]**. The values refers to particle size of $Fe_2O_3.B_2O_3$ nanoparticles is determined to be 22-35 nm, which is close to the measured values by AFM, SEM, and TEM.

### 3.1.3. FESEM of (a) $Fe_2O_3.B_2O_3$ nanoparticles (b) $Fe_2O_3.B_2O_3$-[TBIP]

The morphology of $Fe_2O_3.B_2O_3$ and the nanocomposite $Fe_2O_3.B_2O_3$-[TBIP] was studied using (FESEM) analysis. Through the pictures, we note that$Fe_2O_3$-$B_2O_3$and [TBIP]-$Fe_2O_3.B_2O_3$nanocomposite are shown in Figures3.1(a -b). It shows that $Fe_2O_3$-$B_2O_3$ has rang from 40 to 50 nm, which agrees with the crystallite size determined by XRD data. The morphology of the $Fe_2O_3$-$B_2O_3$ SEM image was similar to that of the AFM image. Still , the clustering-like shape observed resulted in highly agglomerated nanoparticles (cluster mass is made up of tiny particles) that are coherent together.

### 3.1.4. TEM Study of the morphology of the nanocomposite prepared

TEM was used to perform a morphology study on the appearance and average particle size of the manufactured $Fe_2O_3.B_2O_3$ and $Fe_2O_3.B_2O_3$-[TBIP] nanocomposite.TEM images of $Fe_2O_3.B_2O_3$ and $Fe_2O_3.B_2O_3$-[TBIP] nanocomposite before and after $Fe_2O_3.B_2O_3$ adsorption are shown in Figures 3.1(a-b).

### 3. 2.Characterization of compounds [TBIP] , $Fe_2O_3.B_2O_3$ and $Fe_2O_3.B_2O_3$-[TBIP]

### 3.2. 1. (FT-IR)

As shown in Figure(3-2), the FTIR spectrum of compound (a) [TBIP] revealed absorption bands at 3434.56 $cm^{-1}$ for (O-H) stretching vibration, 2955, 2919.05 $cm^{-1}$ for aromatic and aliphatic (C-H) stretching, 1628.36 $cm^{-1}$ for (C=N) stretching, 1050.19 $cm^{-1}$for (C-O) stretching, 1468.19 $cm^{-1}$ for (C-C stretching aromatic), and (1368.36 $cm^{-1}$) for C-N stretching. As shown in Figure 3.2, Moreover, the FTIR spectra of compound (a) [TBIP] showed absorption band at 1050.19 $cm^{-1}$ for (C-S) stretching. Likewise, it can be noticed in FTIRspectra of (b) $Fe_2O_3.B_2O_3$ nanoparticles in figure (3-2) shows the

most important peaks. The stretching of (F-O) at 587.43 $cm^{-1}$ The asymmetric stretching
relaxation of the B–O band of trigonal $BO_3$ units causes the group of bands that arise at 1200–1600 $cm^{-1}$. Figure 3-2 shows the FTIR spectrum of ( c) $Fe_2O_3.B_2O_3$-[TBIP], with band at 3436.33 $cm^{-1}$ due to the presence of asymmetric stretching vibration (N-H), and a band at 2964.05$cm^{-1}$ attributed to aromatic C-H stretching vibration. Other bands at 1637.03, 1470.11, 13861.72, 1261.28, and 1060.36 cm-1 are attributed to gropes (C=N), (C=C) stretching vibration,( =CH) bending vibration, C=S and stretching vibration C–N, respectively.**[12], [13],** as shown in figure (3.2) .

**3.2. 2. $^1$H- NMR of the compound [TBIP]**

$^1$H- NMR spectrum is shown in Figure (3-2)of [TBIP]. It is characterized by the appearance of the signals. The protons which are shown triplet signal in the following methyl group ($CH_3$) at (1.14-1.16) ppm with integration equivalent to (6H), At (1.24-1.28 ppm) with integration equivalent (4H), methylene groups ($CH_2$) are linked with methyl groups ($CH_3$) give hexet signal, methylene groups in aliphatic chain at (1.31 -2.28) ppm with integration equivalent to (68H) give multiple signal ,singlet signal attributed to schiff base protons group (CH=N) at (2.49 -2.80) ppm with integration equivalent (2H) , methoxy groups protons (O-$CH_2$) at (3.13 -3.19) ppm with integration equivalent to (4H) , While protons of group (N-H) at chemical shift (3.9-4.1) ppm appear as a singlet signal with integration equivalent to (2H). The spectrum shows the appearance multiple signal back to aromatic protons represented by (CH) at (6.76-7.32) ppm with integration equivalent to (6H). The last singlet signal with integration equivalent to (2H) is attributed to protons (OH) at (7.8 -7.9) .

**4.1.1. Measurement of the specific conductivity of micelles**

The critical micelle concentration (CMC) of $Fe_2O_3.B_2O_3$-[TBIP] ($4x10^{-4}$), as well as the reduction in conductivity as the nanocomposite surfactant concentration decreases, are depicted in Figure (4-1).This is due the quantity of ions that share electrical properties has decreased , leads to a decreased concentration at a specific point (CMC) with a simple line shift. Because of a minor or no change in conductivity values, it may become a constant value . The development of micelles is indicated at this point.conductivity was measured. CMC values are derived by intersecting the linear sections of the conductivity and surfactant concentration curves.Conductivity in solution is a linear function of counter ion concentration, and the effect grows as counter ion charge density decreases**[14], [15]**.

**4. 1. 2. Measurement of the Hydrophile–Lipophile Balance (HLB)**

Can determine the appropriate type applications of the produced surfactant by comparing the HLB computed values.

$$\mathbf{HLB = 20M_H / M_T} \qquad \text{…… (1)}$$

Where $M_H$ and $M_T$ are the molecular masses of the hydrophilic and total parts of the
molecule, respectively.

We conclude that the prepared nanocomposite $Fe_2O_3.B_2O_3$-[TBIP] is very suitable for working as a surfactant to be used in the treatment of W/O emulsions by calculating the HLB value of the prepared activator, which is equal to (8.1), and comparing it with the standard calculated values from the Griffin equation for surfactants.

The separation efficiency and emulsion stability by using the demulsifier composition of by using equations (2) and (3), respectively.**[16]:**

$$\mathbf{\%\ E_{Separation} = (V_S / V_T) \times 100 \ldots. (2)\ ,}$$

$$\mathbf{\%\ E_{mulsion\ stability} = [1 - (V_S / V_T)] \times 100 \ldots. (3)}$$

Where**:**% $E_{Separation}$**:** The percentage of crude oil water separation efficiency, Vs: separated water volume (ml) and $V_T$**:** Total brine volume in crude oil (2,9 ml)

**4.2. Studying of the Efficiency Separation of $Fe_2O_3.B_2O_3$-[TBIP]as Demulsifier**

The water separation effectiveness of the $Fe_2O_3.B_2O_3$-[TBIP] demulsifier was investigated by treating W/O emulsions for samples taken fromraw petroleum from the Halfaya field , as shown in Table (4.1). In this regard, it should be mentioned that at30°C, The highest value for the separation of water from the emulsion is (51.7%) if the demulsifier concentration is 100 ppm, and the percentage of emulsion stability at this concentration is (48.3%). The lowest (percent $E_{Separation}$) was at a concentration of 50 ppm (13.8%), while the percentage of emulsion stability was (86.2%) at a concentration of 50 ppm. Figure (4.2) illustrates the end outcome diagrammatically. At 60 °C,The quantity of water extracted was (2.3 ml), while the separation

efficiency and emulsion stability were (79.3%) and (20.7 %), respectively in concentration 90 ppm. The lowest percent separation efficiency and the percentage of emulsion stability at a concentration of 50 ppm are (20.7%) and (79.3%), respectively. The result is shown in Figure (4.2).After 90 minutes of testing, a commercial demulsifier (RP96BQ) utilized in Halfaya field crude oil was compared to the synthesized demulsifier$Fe_2O_3.B_2O_3$-[TBIP]in the study to see which was more effective. This comparison shows that the prepared demulsifier's efficiency reached its peak (79.3) at a temperature of 60 °C, whereas the commercial demulsifier's separation efficiency reached 86.2 percent under the same conditions,as shown in Table (4.1).

. At the temperature 60 °C, it is observed that the (% $E_{Separation}$) at a concentration 100 ppm is equal to (% $E_{Separation}$) at a concentration of 90 ppm**,** which is (79.3 %) due to the demulsifier $Fe_2O_3.B_2O_3$-[TBIP], It has diverse impacts on degrading the crude oil interfacial layer as concentration increases, but at a certain point, the pace of layer weakening and the film's resilienceof the film cannot be diminished no matter how highthe concentration is. As a result, the dosage of demulsifier plays a critical function in determining the nature of thecrude oil film.

The $E_{separation}$of the demulsifier $Fe_2O_3.B_2O_3$-[TBIP] with theStandard demulsifier(RP96BQ) used to treat crude oil in Halfaya field is compared, and the dosage of the demulsifier $Fe_2O_3.B_2O_3$-[TBIP] with the commercial demulsifier(RP96BQ) after 90 minutes at both 30 °C and 60 °C temperatures, respectively, is calculated. It can be noted that at both temperatures, the percentage of the separation efficiency of the demulsifier $Fe_2O_3.B_2O_3$-[TBIP] prepared was less than the commercial demulsifier(RP96BQ).Water separation efficiency and Dosage of the demulsifier $Fe_2O_3.B_2O_3$-[TBIP] compared with the commercial demulsifier(RP96BQ) at 30 °C and 60 °Cand the best separation by the nanocompositeDemulsifier, as shown in Figure (4.3).

**Table (2.1): Chemical materials used in this study**

| Substances | Chemical formula | Purity | Company |
|---|---|---|---|
| Hydrazine hydrate | $NH_2NH_2.H_2O$ | 99.9% | /MerckGermany |
| Carbon disulphide | $CS_2$ | 99.9% | UK /Romil |
| Ethanol absolute | $CH_3CH_2OH$ | 99% | /MerckGermany |
| Potassium hydroxide | KOH | 98 % | INDIA/B.D.H |
| 2,5-dihydroxybenzaldehyde | $C_6H_3(OH)_2CHO$ | 98 % | MerckGermany/ |
| 1-Bromoeicosane | $CH_3(CH_2)_{18}CH_2$ Br | 97% | MerckGermany/ |
| Ferrous acetate | $Fe(CH3COO)_2$ | 98% | /MerckGermany |
| Urea | $NH_2CONH_2$ | 99% | India/ SDH |
| Boric acid | $H_3BO_3$ | 95.5% | /MerckGermany |

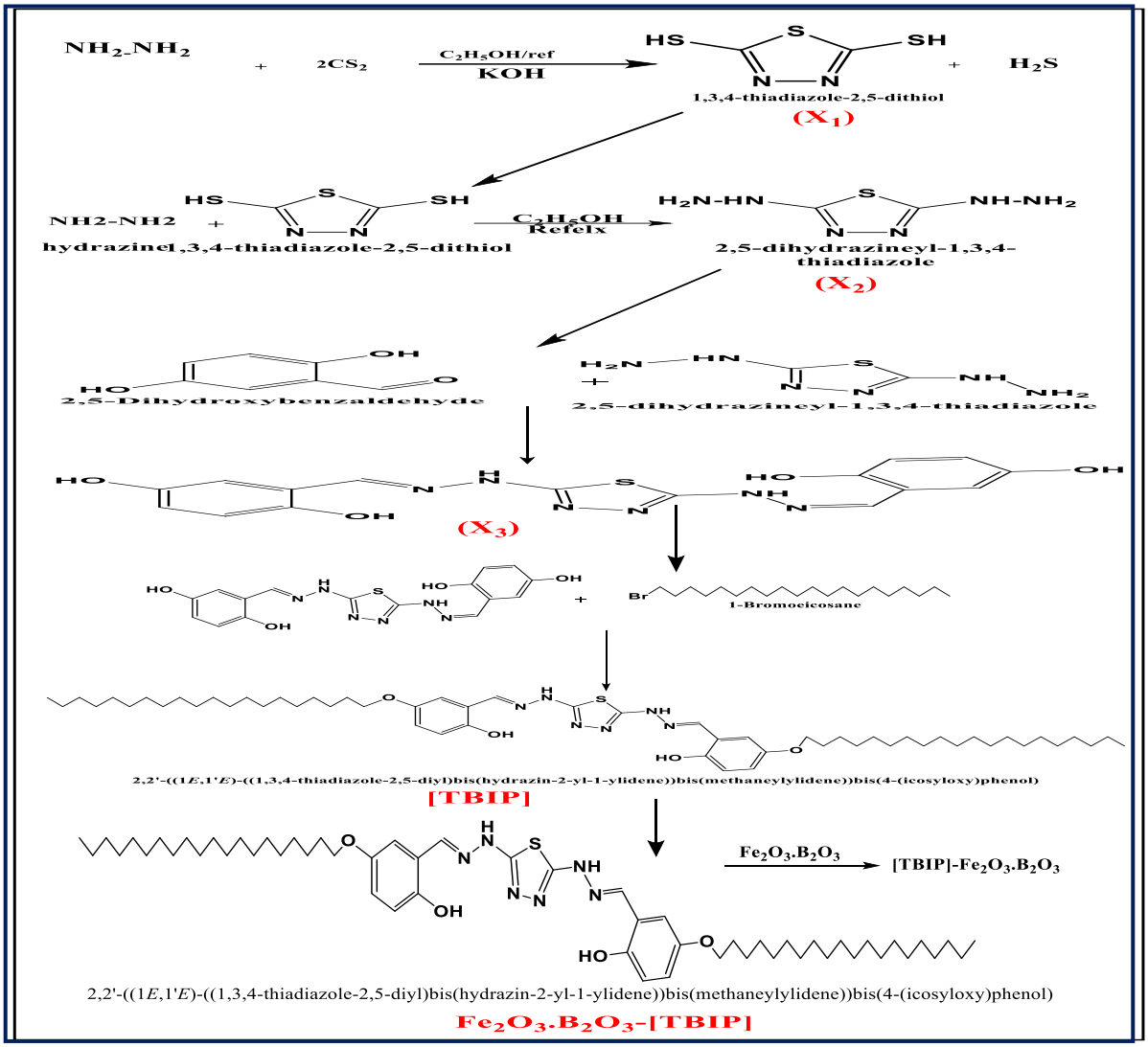


**Scheme. (2.1): Synthesis of nanocomposite$Fe_2O_3.B_2O_3$-[TBIP]**

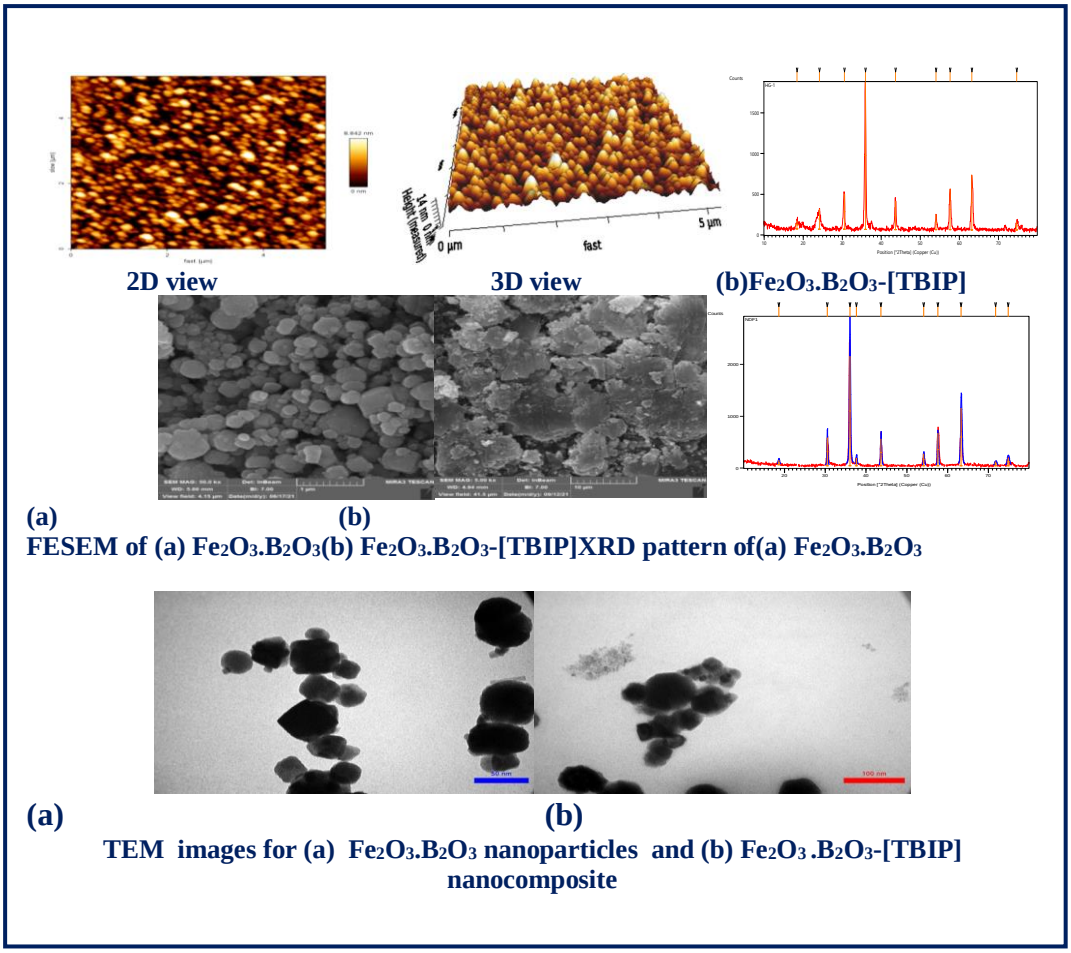


**Figure (3.1):Study of the morphology of the nanocomposite prepared (XRD, FESEM,TEM )**

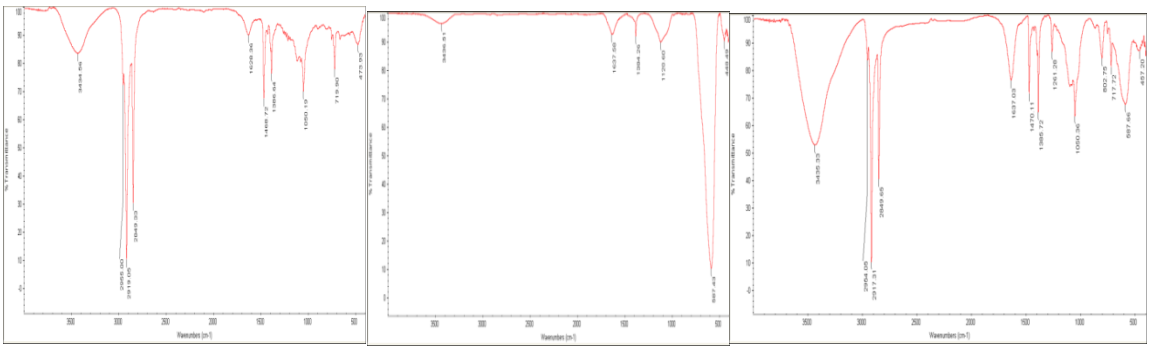

**(a) [TBIP] (b) $Fe_2O_3.B_2O_3$ (c) $Fe_2O_3.B_2O_3$-[TBIP]**

**FT-IR of (a) [TBIP], (b) $Fe_2O_3.B_2O_3$ and (c) $Fe_2O_3.B_2O_3$-[TBIP]**

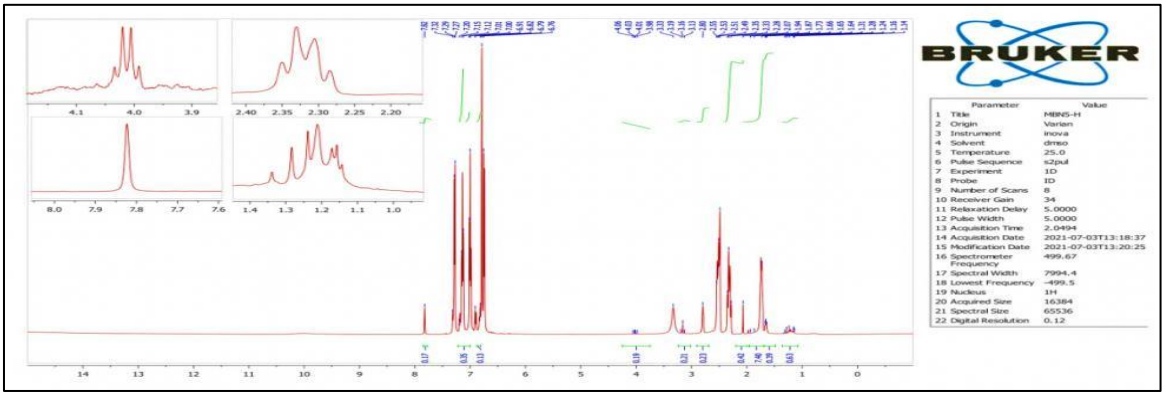


**Figure (3.2): FT-IR and 1H-NMR spectra of [TBIP], $Fe_2O_3.B_2O_3$, and $Fe_2O_3.B_2O_3$-[TBIP] compounds**

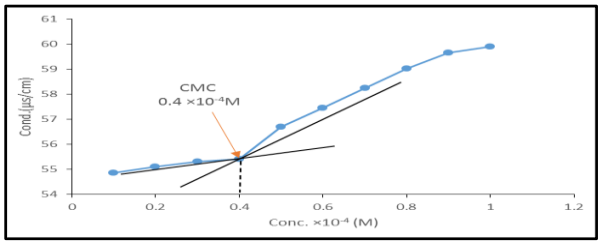


**Figure (4.1): The Relationship between the Changes in Concentration of $Fe_2O_3.B_2O_3$-[TBIP]with Conductivity**

**Table (4.1): Separated Water by Using Demulsifier $Fe_2O_3.B_2O_3$-[TBIP] with Crude Oil of Halfaya field**

| %E Emulsion Stability | %E Separation at 90 min | Water Separated (ml) | | | | | Dosage ppm | Temp (°C) |
|---|---|---|---|---|---|---|---|---|
| | | After 90min. | After 60min. | After 45min. | After 30min. | After 10 min. | | |
| 86.2 | 13.8 | 0.4 | 0.2 | 0.1 | 0.05 | 0 | 50 | 30°C |
| 79.3 | 20.7 | 0.6 | 0.4 | 0.3 | 0.1 | 0.05 | 60 | |
| 75.9 | 24.1 | 0.7 | 0.6 | 0.4 | 0.2 | 0.1 | 70 | |
| 72.4 | 27.6 | 0.8 | 0.7 | 0.6 | 0.4 | 0.2 | 80 | |
| 65.5 | 34.5 | 1 | 0.9 | 0.7 | 0.5 | 0.2 | 90 | |
| 48.3 | 51.7 | 1.5 | 1.1 | 1 | 0.7 | 0.4 | 100 | |
| 79.3 | 20.7 | 0.6 | 0.4 | 0.3 | 0.1 | 0 | 50 | 60°C |
| 72.4 | 27.6 | 0.8 | 0.6 | 0.4 | 0.2 | 0.05 | 60 | |
| 65.5 | 34.5 | 1 | 0.9 | 0.7 | 0.3 | 0.2 | 70 | |
| 58.6 | 41.4 | 1.2 | 1 | 0.9 | 0.5 | 0.3 | 80 | |
| 20.7 | 79.3 | 2.3 | 1.5 | 1.2 | 0.6 | 0.4 | 90 | |
| 20.7 | 79.3 | 2.3 | 1.8 | 1.6 | 0.9 | 0.6 | 100 | |

**Table (4.2):Separated Water by Using Standard CommercialDemulsifier(RP96BQ) with Crude Oil of Halfaya field**

| %E Emulsion Stability | %E Separation at 90 min | Water Separated (ml) | | | | | Dosage ppm | Temp (°C) |
|---|---|---|---|---|---|---|---|---|
| | | After 90min. | After 60min. | After 45min. | After 30min. | After 10 min. | | |
| 93.1 | 6.9 | 0.2 | 0.1 | 0.05 | 0.05 | 0 | 50 | 30°C |
| 75.9 | 24.1 | 0.7 | 0.3 | 0.1 | 0.05 | 0 | 60 | |
| 65.5 | 34.5 | 1 | 0.4 | 0.2 | 0.05 | 0.05 | 70 | |
| 55.2 | 44.8 | 1.3 | 0.8 | 0.6 | 0.4 | 0.1 | 80 | |
| 34.5 | 65.5 | 1.9 | 1.4 | 0.8 | 0.5 | 0.3 | 90 | |
| 34.5 | 65.5 | 1.9 | 1.5 | 1.2 | 0.8 | 0.6 | 100 | |
| 75.9 | 24.1 | 0.7 | 0.4 | 0.2 | 0.1 | 0.05 | 50 | 60°C |
| 72.4 | 27.6 | 0.8 | 0.5 | 0.3 | 0.1 | 0.1 | 60 | |
| 58.6 | 41.4 | 1.2 | 0.7 | 0.6 | 0.4 | 0.1 | 70 | |
| 48.3 | 51.7 | 1.5 | 1 | 0.9 | 0.7 | 0.3 | 80 | |
| 13.8 | 86.2 | 2.5 | 1.6 | 1 | 0.8 | 0.7 | 90 | |
| 13.8 | 86.2 | 2.5 | 1.8 | 1.6 | 1.3 | 0.9 | 100 | |

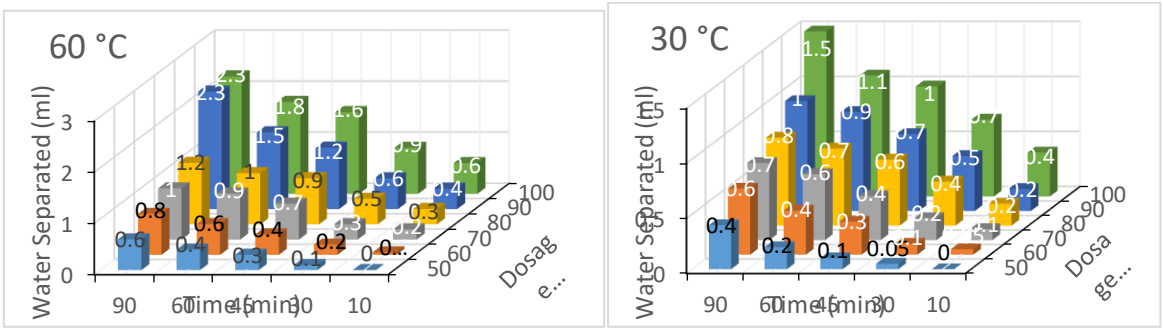


**Figure( 4.2): The effect of the change in time and temperature in the presence of the prepared demulsifier on the efficiency of water separation from petroleum emulsions**

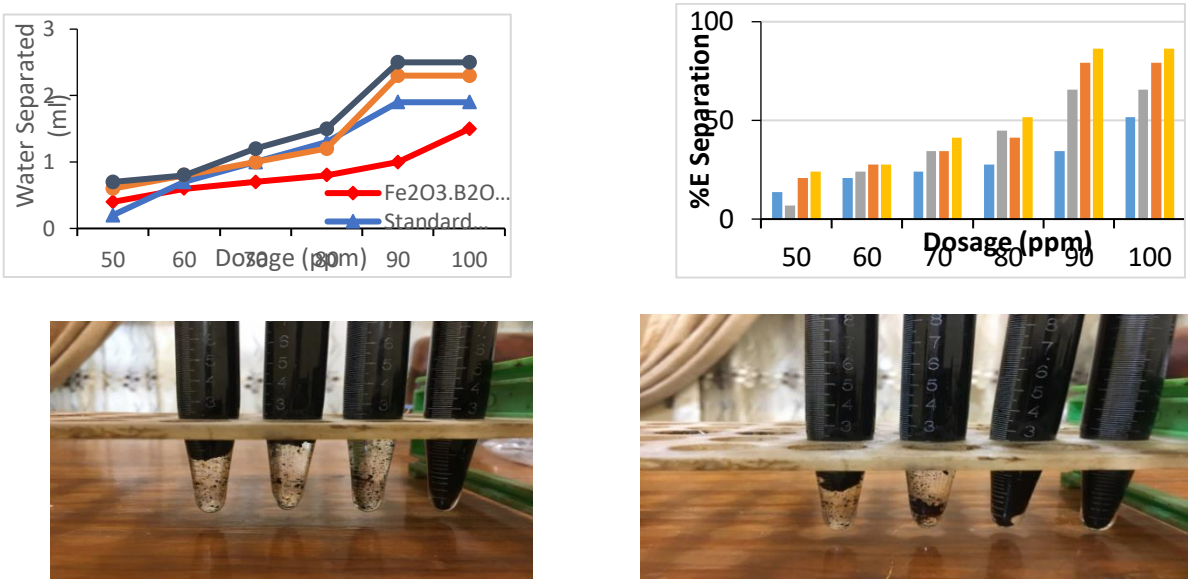


**Figure (4.3): Comparison of the separation efficiency between the prepared nanodemulsifier and the standard demulsifier(RP96BQ)**

### 4.2. 1. Concentration's Impact

The concentration of surfactants in the nanocomposites produced, which is one of the most important properties of demulsifiers $Fe_2O_3.B_2O_3$-[TBIP], has a significant impact on crude oil separation efficiency.When compared to the lowest concentrations of 50, 60, 70, and 80 ppm, a concentration of 90 ppm was shown to have a high separation efficiency in a short amount of time. The greater the concentration, the more demulsifier molecules are adsorbed onto the water/oil interface, causing variations in interfacial tension or film pressure. Finally, the rate of film thinning (drainage) is increased while its stability is decreased, making the interfacial layer that holds water drops easier to dissolve. As a result, the emulsion separates into two phases. It takes the most time to attain the same separation efficiency when working with low concentrations as when working with high concentrations[17**]**.

### 4.2. 2. Effect of Temperature

Separating water from crude oil as an emulsion (W/O) performed well at 30°C, but it took longer. At 60°C, the separation process is efficient, and a huge amount of water can be separated in a matter of minutes. As a result, it is plausible to assume that temperature has a significant effect on liquid surface tension, which decreases with increasing temperature. As a result, rather than the natural emulsifier, the demulsifier molecules are easily associated with the emulsion molecule drop interface, diffusion, and penetration absorption,resulting in the production of a positive tension gradient. A lower water interfacial film is formed in comparison to the poor mixed film's stability. As a result, as the temperature rises, the separation efficiency falls **[18].**

### 4.2. 3. Time effect

Because the demulsifier spread between emulsion (W/O) droplets increases over time, so does the separation efficiency of $Fe_2O_3.B_2O_3$-[TBIP] **prepared**demulsifier, As a result, the demulsifier is exposed to a wider surface area.This depicts the point of demulsifier-emulsion convergence at the critical point where the film begins to deteriorate around a droplet**[19]**. Because the molecules that experience adsorption become bound with the surface atoms, the free energy (ΔG) and entropy (ΔS) decrease, and this is accompanied by a decrease in enthalpy (ΔH) **[20]** depending on the equation (4) **:**

$$\Delta G = \Delta H - T\Delta S \qquad \text{.....(4)}$$

### 4.3. Conclusions

This research could lead to the following conclusions:

1.The effectiveness of water separation improves proportionately with the dosage of the synthesized demulsifier $Fe_2O_3.B_2O_3$-[TBIP].], with a concentration of 90 ppm having a higher separation

efficiency in a shorter time than the lower concentrations (50, 60, 70, and 80) ppm.

2**.** At lower concentrations, high temperatures result in enhanced separation efficiency, which increases as the temperature rises.

3.For $Fe_2O_3.B_2O_3$-[TBIP] demulsifier, The effectiveness of water separation improves as separation time increases, with the best separation achieved at (90 min).

4. At both 30 °C and 60 °C, the separation efficiency of the synthesized nano-demulsifier $Fe_2O_3.B_2O_3$-[TBIP] was comparable to that of the commercial demulsifier. It is a separation efficiency approach for the commercial demulsifier that is employed, so thatthenanocomposite synthesizedcan be used as a water/oil demulsifier.

**Refrences**


[1] Y. Gogotsi, *Nanomaterials*. United States of America on: Taylor & Francis, 2006.

[2] M. Bonazzi, *Nanotechnologies: Principles, Applications, Implications and Hands-on Activities*. 2013.

[3] H. Yagoub *et al.*, "Complex membrane of cellulose and chitin nanocrystals with cationic guar gum for oil/water separation," *J. Appl. Polym. Sci.*, vol. 136, no. 37, pp. 1–10, 2019.

[4] S. O. Olayiwola and M. Dejam, "A comprehensive review on interaction of nanoparticles with low salinity water and surfactant for enhanced oil recovery in sandstone and carbonate reservoirs," *Fuel*, vol. 241, no. October 2018, pp. 1045–1057, 2019.

[5] T. Mi *et al.*, "Synthesis of Fe3O4 nanocomposites for efficient separation of ultra-small oil droplets from hexadecane-water emulsions," *RSC Adv.*, vol. 10, no. 17, pp. 10309–10314, 2020.

[6] V. T. Tan, L. The Vinh, L. Tu Quynh, H. Thu Suong, and H. Dang Chinh, "A novel synthesis of nanoflower-like zinc borate from zinc oxide at room temperature," *Mater. Res. Express*, vol. 7, no. 1, pp. 1–9, 2020.

[7] N. A. Basher, I. A. Flifel, and A. A. Mashaf, "Synthesis, Characterization and antibacterial Study of some Complexes Derivatives from1,3,4-Thiadiazole Schiff base," *IOP Conf. Ser. Mater. Sci. Eng.*, vol. 928, no. 5, pp. 1–15, 2020.

[8] N. A. Basher, "Study of New Derivatives of 1,3,4-Thiadiazole and Its Complexes with chromium ion (Cr+3)," *IOP Conf. Ser. Mater. Sci. Eng.*, vol. 928, no. 5, pp. 1–13, 2020.

[9] A. N. Ayyash, H. J. Jaffer, and J. H. Tomma, "Synthesis and characterization of some novel 4-thiazolidinones and isoxazolines derived from thiosemicarbazones," *Am. J. Org. Chem.*, vol. 4, no. 2, pp. 52–62, 2014.

[10] O. A. Adeyanju and L. O. Oyekunle, "Optimum demulsifier formulations for Nigerian crude oil-water emulsions," *Egypt. J. Pet.*, vol. 27, no. 4, pp. 657–662, 2018.

[11] J. S. Justus, S. D. Dharma Roy, K. Saravanakumar, and A. M. Ezhil Raj, "Judging phase purity of hematite (α-Fe2O3) nanoparticles through structural and magnetic studies," *Mater. Res. Express*, vol. 8, no. 5, pp. 1–16, 2021.

[12] D. J. Pérez Martínez, G. A. A. Quiroga, S. A. G. Duarte, and A. C. Hurtado, "Surface characterization of borated γ-alumina by using proton affinity distributions | Caracterización de la superficie de γ-alúminas modificadas con boro usando distribuciones de afinidad protónica," *Rev. Fac. Ing.*, no. 57, pp. 23–30, 2011.

[13] V. Kundu, R. L. Dhiman, A. S. Maan, and D. R. Goyal, " Structural and Physical Properties of Fe2O3-B2O3-V2O5 Glasses ," *Adv. Condens. Matter Phys.*, vol. 2008, no. January 2008, pp. 1–7, 2008.

[14] A. Domínguez, A. Fernandez, N. Gonzalez, E. Iglesias, and L. Montenegro, "Determination of Critical Micelle Concentration of Some Surfactants by Three Techniques," *J. Chem. Educ.*, vol. 74, pp. 1227–1231, 1997.

[15] M. B. and Q. C. Y. Li, H. Zhang, "Aggregation Behavior of Surfactants with Different Molecular Structures in Aqueous Solution: DPD Simulation Study," *J. Dispers. Sci. Technol.*, vol. 33, pp. 1437–1443, 2012.

[16] Ali Abdulkhabeer Ali, Ali Abdul Hakeem Naghmash, " Evaluation of the effectiveness of synthesized polymeric demulsifiers in the petroleum sector", solid state technology., Vol 63,issu 2,pp. 1294-1307,2020.

[17] A. Alsabagh, M. E. Hassan, and S. E. M.

Desouky, “Demulsification of W/O emulsion at petroleum field and reservoir conditions using some demulsifiers based on polyethylene and propylene oxides.,” *Egypt. J. Pet.*, vol. 25, no. 4, pp. 585–595, 2016.

[18] R. Zolfaghari, A. Fakhru’l-Razi, L. C. Abdullah, S. S. E. H. Elnashaie, and A. Pendashteh, “Demulsification techniques of water-in-oil and oil-in-water emulsions in petroleum industry,” *Sep. Purif. Technol.*, vol. 170, pp. 377–407, 2016.

[19] G. I. Kelbaliev and F. F. Safarov, “Study of interphase film thinning in petroleum emulsion separation processes,” *J. Chem. Technol. Fuels Oils*, vol. 47, no. 4, pp. 268–277, 2011.

[20] T. F. Tadros, *Applied Surfactants, Principles and Applications*, 1st Editio. Germany: Wiley-VCH Verlag GmbH and Co. KGaA, 2005.